



# Characteristics of a Large-Scale Deep Foundation Pit Excavated by the Central-Island Technique in Chengdu Soft Clay

Dongxing Ren<sup>a</sup>, Chao Kang<sup>b,c</sup>, Huanhuan Liu<sup>d</sup>, Yin Li<sup>a</sup>, and Jilin Wang<sup>a</sup>

<sup>a</sup>Chengdu Surveying Geotechnical Research Institute Co., Ltd. of MCC, Chengdu 610023 China

<sup>b</sup>School of Engineering, Huanghe Science and Technology University, Zhengzhou 450000, China

<sup>c</sup>School of Engineering, University of Northern British Columbia, Prince George V2N 4Z9, Canada

<sup>d</sup>Sichuan Energy Saving and Environmental Protection Investment Co., Ltd., Chengdu 610023, China

## ARTICLE HISTORY

Received 10 June 2021  
Revised 29 November 2021  
Accepted 10 January 2022  
Published Online 24 March 2022

## KEYWORDS

Large-scale foundation pit  
Excavation behaviours  
Anchor cables  
Central island technique  
Soft clay

## ABSTRACT

A large-scale foundation pit, 25,720 m<sup>2</sup> (127 m × 213 m), was excavated to a depth of approximately 20 m by the central-island technique from 2012 to 2013 in Chengdu, China. This paper aims to comprehensively study the deformation behaviours of the foundation pit during excavation and investigate the primary factors affecting the deformation behaviour of the foundation pit. The deformation characteristics monitored during excavation included 1) horizontal column movement, 2) vertical column movement, 3) lateral column deflection, 4) internal stress in the column, 5) axial force in anchor cables, 6) ground settlement, and 7) artesian water levels. To further explore the pit sizes on the excavation behaviour, field data from another ten excavations in Chengdu were also included in the analysis. The results showed the maximum deflection of the column was mostly detected at the top of the column. The vertical column movement,  $\delta_{v1}$ , undulates during excavation. After the desired depth was reached, the increase in the vertical column movement was negligible. The internal force in the anchor cable varied between 20 – 30 kN during the excavation and between 30 – 70 kN when the expected depth was excavated. A relatively small ground settlement in the studied excavation sites was observed due to the mudstone at the bottom of the excavation and the installation of anchor cables. In addition, it was noticed that the aspect ratio and excavation depth have a significant effect on the maximum deflection at the top of the column. This paper enriches the database and improves the understanding of the deformation behaviour of large-scale foundation pits during excavation.

## 1. Introduction

In the past decades, more and more large size open foundation pits were constructed benefiting from the development of design knowledge and construction techniques, e.g., open pits for metro line #4 in Shanghai (40.9 m in depth), laboratory testing pit in Shanghai Jiaotong University (39 m in depth), etc. (Li, 2012). Bottom-up and top-down methods were in general adopted for the excavation of the large size foundation pits. For the top-down approach, excavation has to be conducted after installing the internal structure, which was temporarily used to support the diaphragm wall (Finno et al., 1989; Tan and Wang, 2013a). For the bottom-up method, temporary struts were used to prevent the failure of

the pits, e.g., temporary diaphragm wall and the construction started from the bottom and worked upwards (Tan and Wang, 2013b). Due to the size of large-scale foundation pits, the central-island technique was adopted for most of the large-scale excavations, where the center of the soil was first excavated while the soil close to the boundary of the foundation pit was not excavated to provide supporting force to diaphragm walls.

The deformation behaviours during excavation had to be monitored to prevent the potential failure of the foundation pits before the completion of construction. In general, there are three approaches to estimate the possible ground settlement, including empirical approach, physical modelling, and numerical simulation. Several empirical models have been proposed to estimate the

**CORRESPONDENCE** Chao Kang ✉ chao.kang@unbc.ca 📧 School of Engineering, Huanghe Science and Technology University, Zhengzhou 450000, China; School of Engineering, University of Northern British Columbia, Prince George V2N 4Z9, Canada

excavated-induced wall deflection and surface settlement (Peck, 1969; Clough, 1990; Ou et al., 1993; Hashash and Whittle, 1996; Hsieh and Ou, 1998). The wall deflection, vertical column movement and ground settlement were generally correlated to the excavation depths through a linear relationship. The upper boundary of the coefficient for the relationship between maximum wall deflection and excavation depth was 1.0% (Peck, 1969), and that between maximum column movement and excavation depth was 0.20% (Tan and Wang, 2013a). The ground settlement was relatively larger compared with maximum column movement which was correlated to excavated depth with a maximum ratio of 0.50%. However, several factors can limit the application of the proposed empirical correlations, including the arching effect at the corner section for rectangular pits, involvement of underground water, layered soil conditions, type of supporting structures, and the excavation depth (Ou et al., 1993; Yi et al., 2015). Therefore, the empirical correlation was generally proposed for small regions with similar soil conditions and excavation strategies. However, the proposed empirical correlations can still be used in the design stage as they were straightforward.

The approach of the physical simulation was adopted to study the bearing capacity and settlement behaviour of foundations. Small-scale laboratory physical models were generally constructed, as the full-scale field test was very costly (Eid et al., 2009). However, the scale effect was always one of the main concerns when applying the results to real projects, which can be significant when a retaining wall was used in the model (Eid et al., 2009). The advantage of the physical simulation was that complicated soil conditions could be considered in the study. Centrifuge model tests can overcome this difficulty by simulating the deformation behaviour of field excavations in a small-scale model through creating similar conditions (i.e., stability number) (Takemura et al., 1999). Many tests on excavations in clay and sand have been conducted using centrifuge tests (Ng et al., 2013; Zhang et al., 2020).

Numerical simulation is another approach that can be used to predict wall deflection and ground settlement resulting from the excavation. In general, the finite element method was adopted

with implementing elastoplastic constitutive models (Clough and Hansen, 1981; Kung et al., 2009), which was benefited from advances in computer hardware, software capabilities and economic and legal pressure (Hashash et al., 2006). However, because of the non-linear behaviour of clay and the limitation of obtaining soil parameters at small strain, the calculated surface settlement near the retaining wall and that observed has a significant discrepancy (Hsieh and Ou, 1998).

Although many empirical or semi-empirical correlations have been proposed to predict the excavation behaviours for bottom-up and top-down methods, most of them were developed based on small-scale excavations. Due to the development of design methods and construction techniques, open pits in recent decades have become larger and deeper. In addition, pit size has an impact on the excavation behaviour. Thus, an improved correlation is expected to estimate the ground-surface settlement and wall deflection of large-scale excavations.

This paper presents the investigated results of a large-scale excavation of Chengdu Universal Trade Plaza (CDUTP) foundation pits. The primary monitored deformation characteristics include displacements, i.e., lateral deflection of the columns, vertical and horizontal movement during monitoring and ground settlement, forces, i.e., the internal force in the anchor cable and stress in the column, and pore water pressure. The correlation between excavation depth and corresponding monitoring indices used to describe excavation behaviour is evaluated based on the monitored results. To investigate the impact of pit size on the excavation behaviours, the information regarding excavation behaviours from another ten foundation pits in Chengdu is also included for comparison. This paper provides detailed knowledge of the excavation of a large-scale deep foundation pit, which can improve the understanding of the excavation behaviours of large-scale foundation pits.

## 2. Site Description

### 2.1 Bottom-Up Construction of the Rectangular Pit

Figure 1 shows the layout of the construction site as well as the

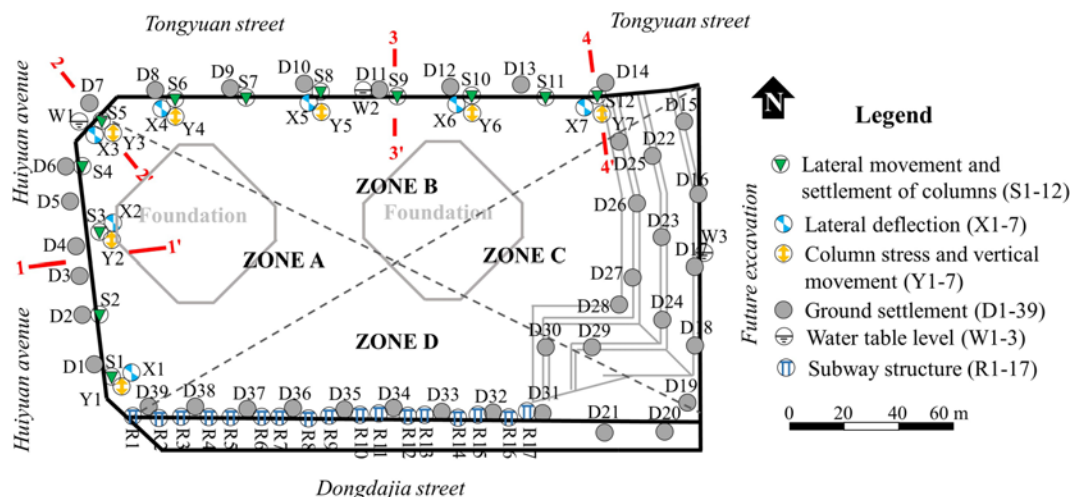


Fig. 1. Instrumentation and Monitoring Points of the Rectangular Pit

locations of monitoring instruments along the boundary of open pits. The width and length of the pit were 127 m and 213 m, respectively, and the total excavation area was approximately 25,720 m<sup>2</sup>. During excavation, deformation characteristics, including ground settlement, column movement, compression stress in the columns and internal force in anchor cables, were monitored. Most of the monitoring points were designed along the boundaries of the pit (Fig. 1). Some of them were placed on the temporary

structures used for the excavation of an adjacent pit.

Before the construction of the structures, the foundation pit was excavated to reach an expected depth. The excavation of the pit started with the construction of the concrete pile wall. For the central-island technique, the excavation began at the central portion of the pit (Tan and Wang, 2013a), leaving the soil close to the columns until the installation of the anchor cables is completed, which can advance the construction rate. Generally,

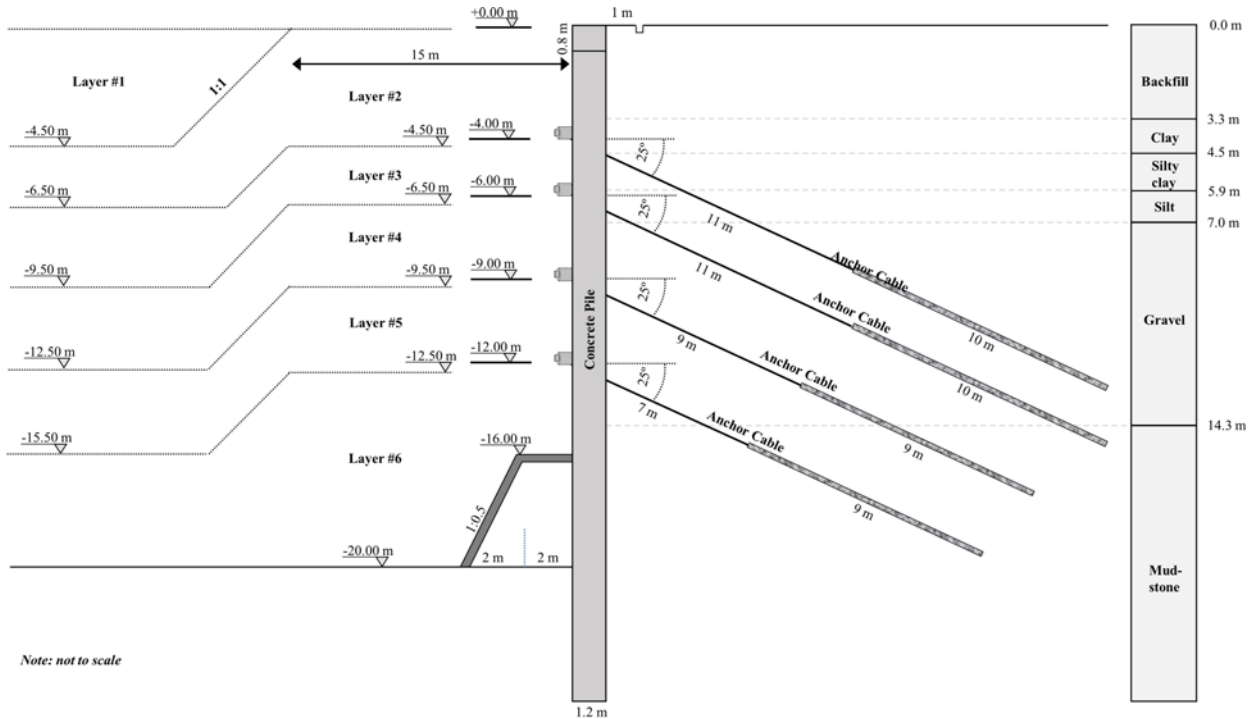


Fig. 2. Typical Cross Section of the Rectangular Pit and Corresponding Soil Types (section 3-3 in Fig. 1)

Table 1. Table Main Construction Stages of the Foundation Pits

Stages	Event	Date (mm/dd/yyyy)	
		Zone A	Zone B
1	Construction of the diaphragm wall and concrete piles around the pit.	03/10/2012 – 04/05/2012	03/06/2012 – 04/08/2012
2	Excavation of Soil Layer #1 at the center of the pit to a depth of 4.5 m BGS.	06/02/2012 – 06/03/2012	05/25/2012 – 06/18/2012
3a	Excavation of the Soil Layer #2 to a depth of 4.5 m BGS. Meanwhile, the center part of the pit was excavated to a depth of 6.5 m BGS.	06/04/2012 – 06/21/2012	05/27/2012 – 06/20/2012
3b	Installation of the first layer of anchor cables and curing of the cast slabs.	06/26/2012 – 07/27/2012	2012.06.11 – 2012.07.29
4a	Excavation of the Soil Layer #3 to a depth of 6.5 m BGS. Meanwhile, the center part of the pit was excavated to a depth of 9.5 m BGS.	08/20/2012 – 09/01/2012	08/15/2012 – 08/27/2012
4b	Installation of the second layer of anchor cables and curing of the cast slabs.	09/02/2012 – 09/23/2012	08/28/2012 – 09/18/2012
5a	Excavation of the Soil Layer #4 to a depth of 9.5 m BGS. Meanwhile, the center part of the pit was excavated to a depth of 12.5 m BGS.	09/25/2012 – 09/27/2012	09/18/2012 – 09/21/2012
5b	Installation of the third layer of anchor cables and curing of the cast slabs.	09/28/2012 – 10/14/2012	09/22/2012 – 10/06/2012
6a	Excavation of the Soil Layer #5 to a depth of 12.5 m BGS. Meanwhile, the center part of the pit was excavated to a depth of 15.5 m BGS.	10/20/2012 – 10/23/2012	10/04/2012 – 10/08/2012
6b	Installation of the fourth layer of anchor cables and curing of the cast slabs.	10/24/2012 – 11/04/2012	10/08/2012 – 10/29/2012
7	Excavation of the Soil Layer #6 to the final depth of 20 m BGS.	12/08/2012 – 02/27/2012	12/12/2012 – 02/27/2013
8	Construction of underground structures	03/28/2013 – 10/28/2013	03/28/2013 – 10/28/2013

Note: BGS denotes below ground surface.

the central island technique was adopted for large-scale foundation pit in Chengdu due to the relatively good soil conditions, which was adopted during excavation for this foundation pit as well, see Fig. 2. From Layer #2 to Layer #5, after reaching the designed depth, anchor cables were installed and cured before the deformation was stable. Then, the excavation for the following stages started. The excavation was begun on March 1, 2012, and reached the expected depth for the entire foundation pit on February 27, 2013. Table 1 lists detailed construction activities for each region in Fig. 1. Since Zone C is close to the future excavation site and Zone D is close to a subway monitored through R1-R17, the detailed construction information was not recorded.

## 2.2 Instrumentation

In general, monitoring the deformation of soil along with the pit, movement of the columns, and stress and force in the column and anchor cables, are part of the work required for safe excavation of a pit. In addition, the data can be used to investigate excavation behaviours further. Fig. 1 displays the layout of the instrument in the plan. The monitored items are 1) column deflections measured by inclinometer (YKCX-7330) (designed as X1-X7); 2) axial

force in the steel used in the concrete pile measured by vibrating wire stress meters (YKMS-2101) (designed as X1-X7); 3) stress in the anchor cables (4, 9 and 12 m below ground surface) measured using dynamometer (YKMS-3201IT) (designed as Y1-Y7); 4) ground settlement surveyed at 39 stations along the boundary of the pit measured using total station (designed as D1-D39); 5) subsurface settlements behind the wall of the pit using the total station as well (R1-R17); 6) vertical column movement using total station (S1-S12); and 7) phreatic water table levels measured by three standpipes (designed as W1-W3).

## 2.3 Site Subsurface Conditions

Before the construction, the soil properties were explored at more than 255 locations by a series of field tests, including standard penetration tests and field wave velocity tests, and laboratory tests (Atterberg limit tests, swelling test, permeability test and direct shear test). Fig. 3 shows the soil profiles and soil properties obtained from field and laboratory tests. Since the construction site was extensive, the thickness of soil layers varied in space. Therefore, the average thickness of soil layers was plotted.

According to borehole information, it was noticed that most of the excavation happened in clay. When close to the bottom of

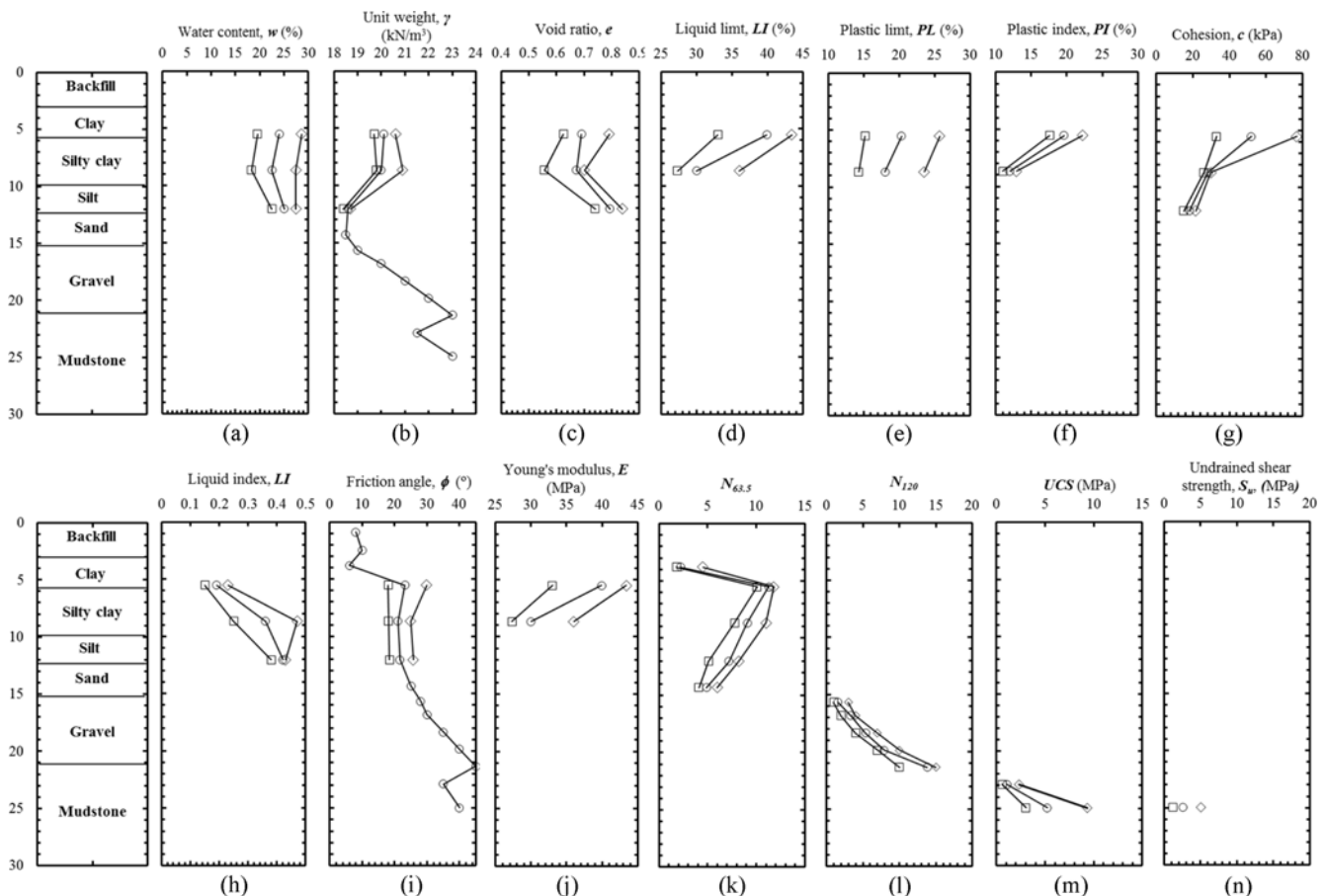


Fig. 3. Available Physical and Mechanical Properties of Soil: (a) Water Content, (b) Unit Weight, (c) Void Ratio, (d) Liquid Limit, (e) Plastic Limit, (f) Plastic Index, (g) Cohesion, (h) Liquid Index, (i) Friction Angle, (j) Young's Modulus, (k) SPT  $N_{63.5}$  Value, (l) Modified SPT  $N_{120}$  Value, (m) Unconfined Compression Strength, (n) Undrained Shear Strength

the open pit, sand and gravel were observed. At some locations, mudstone was even observed. Therefore, no need to monitor the heaving of the foundation bottom in the following construction stages. Based on the field and laboratory test results, the mechanical properties of soil in Fig. 3 were used in the design of piles and reinforcement structures.

### 3. Field Measurement

#### 3.1 Lateral Movement along the Column

Figure 4 summarizes the available lateral movement along with the monitored columns. The column developed the maximum movement at the top of the column most of the time. Since the

column located at X3 is at the corner of the two boundaries, the lateral movement was only approximately half of that observed in columns located at X1, X2, X4, X5, X6, and X7, which were close to 20 mm at the end of the excavation. The limited deflection at location X3 was due to boundary conditions at the north and west sides of the foundation pits, which has been explained in detail by Liu et al. (2021a). Most of the lateral movement was detected in Stages 5 and 6 as the excavation was close to the expected depth. The reason for the maximum movement observed at the surface is that the column with high strength develops less deflection in the column. Another reason is that the soil at the bottom of the pit was gravel and mudstone, which have higher strength based on Fig. 3. This can be verified

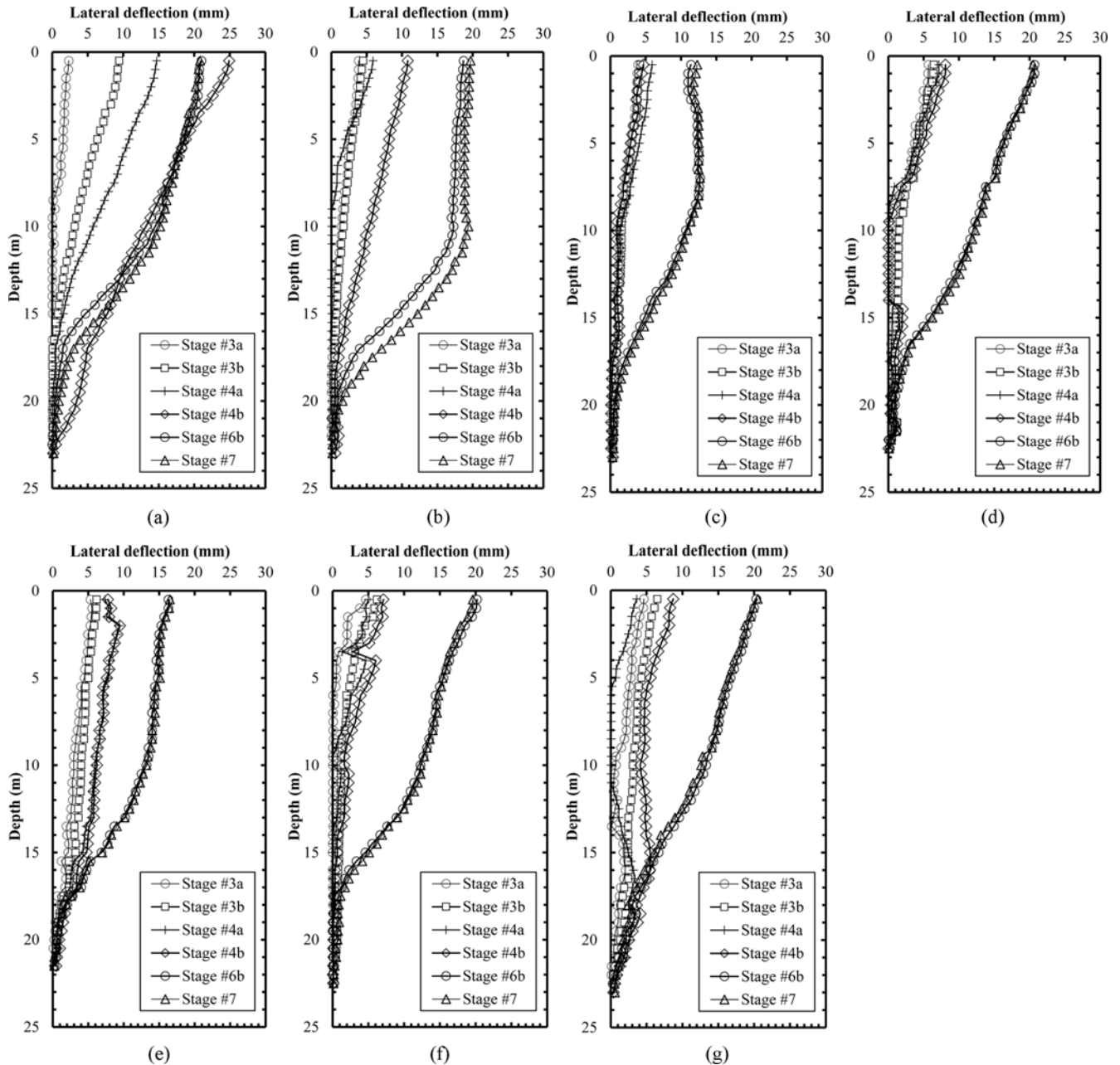


Fig. 4. Summary of Available Lateral Column Deflection at Points: (a) X1, (b) X2, (c) X3, (d) X4, (e) X5, (f) X6, (g) X7

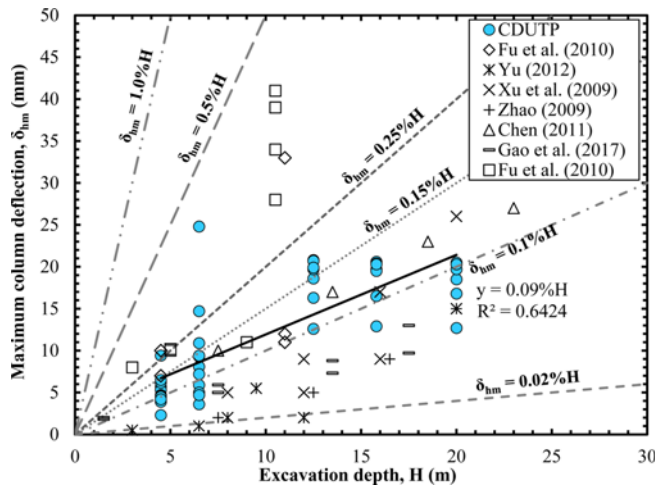


Fig. 5. Relationship between  $\delta_{hm}$  and  $H$

based on the measured deflection close to the bottom of the excavation, which reduced dramatically.

Figure 5 shows the relationship between the maximum wall deflection,  $\delta_{hm}$ , and the excavation depth,  $H$ . The maximum wall deflection,  $\delta_{hm}$ , was the maximum deflection along a column when a certain depth was reached. To better understand the behaviours of the rectangular pit, data from another seven pits with similar soil conditions in Chengdu is also included here to investigate the deformation characteristics. As shown in Fig. 5, the relationship between  $\delta_{hm}$  and  $H$  for this study is mostly between lines of  $\delta_{hm} = 0.02\%H$  and  $\delta_{hm} = 0.25\%H$ . The trend line for this case falls between  $\delta_{hm} = 0.1\%H$  and  $\delta_{hm} = 0.15\%H$ . The measured  $\delta_{hm}$  was close to the lower boundary of basement excavation in Tan and Wang (2013b). Although the excavation site was relatively large, the wall deflection was comparatively small, which was associated with the installation of anchor cables. In addition, the diameter of the concrete column effectively limited the wall deformation. If compared with the proposed correlation between  $\delta_{hm}$  and  $H$  for soft soils, the measured  $\delta_{hm}$  in this study was far below the upper boundary of Clough (1990) ( $\delta_{hm} = 0.5\%H$ ), Kung et al. (2007) ( $\delta_{hm} = 0.6\%H$ ), and Peck (1969) ( $\delta_{hm} = 1.0\%H$ ). The measured  $\delta_{hm}$  in this study was even smaller than the lower boundaries proposed by Clough (1990) ( $\delta_{hm} = 0.22\%H$ ), and Kung et al. (2007) ( $\delta_{hm} = 0.2\%H$ ). For the rest of the available cases, the relationship between  $\delta_{hm}$  and  $H$  was still close to  $\delta_{hm} = 0.15\%H$ , which was still relatively small and below the lower boundaries proposed by Clough (1990) and Kung et al. (2007). Small wall deflection was due to the bottom-up excavations showing a capacity for resisting deformation. Another reason was the soil with high strength at the bottom of the excavation can provide a high supporting force to prevent the deformation of the column, which can be verified by the measured stress in the column.

Different from the monitored lateral deflection of the other deep-seated excavations, which have the maximum deflection observed at the half depth of the wall (Tan and Wang, 2013a), the maximum observed deflection was always observed at the top of

the column, which was consistent with other reported cases in Chengdu area (Fu et al., 2010; Yu, 2012; Gao et al., 2017). The limited deformation was attributed to the stiffness of the supporting systems (i.e., wall bending stiffness, location of anchor cable, etc.), which were capable of resisting lateral deflection. However, the effect of the supporting systems should be studied by comparing the maximum lateral deflection of the foundation pits with and without supporting structures.

### 3.2 Column Movement and Internal Stress

The column might move horizontally and vertically during the excavation of the foundation pit. Fig. 6 shows the development of the column displacement, which was measured at the top of the column. Fig. 6(a) presents the movement of the top of the column perpendicular to the excavation surface, whilst Fig. 6(b) shows the movement along the boundary of the pit. In the initial stages, e.g., Stages #1 and #2, there was no movement in the horizontal plane as soil close to the column had not been excavated. However, after that, the horizontal displacement developed, and the increase of the movement was also linear with the progress of the excavation, resulting from the removal of the soil close to the

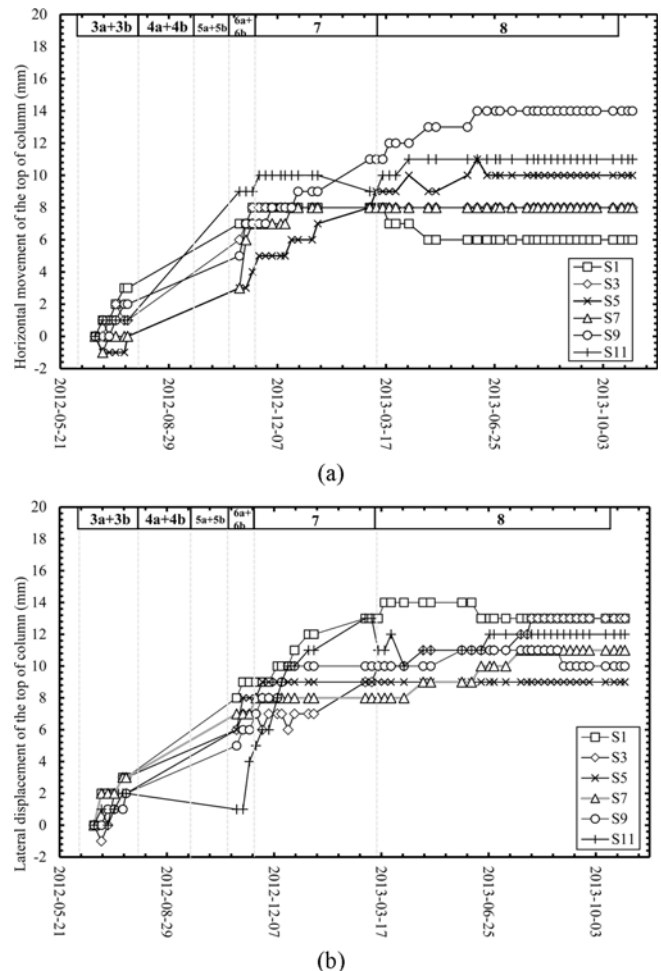


Fig. 6. Typical Development of Column Behaviours with Time: (a) Horizontal Column Movement, (b) Lateral Displacement at the Top of the Column

column. After the completion of excavation and the installation of anchor cables, there was no noticeable movement detected in the horizontal plane. The maximum movement of all monitored points was about 14 mm in both directions. Once the soil had been moved in Stage 7, an increase in the movement was detected. However, after a short period, no additional horizontal movement was detected, which was due to releasing stress had finished, and force from anchor cables limited the movement of the soil. The anchor cable close to the base of the foundation pit was installed in the sand and gravel, which can provide a relatively large resistance force to the lateral and horizontal movements of the columns.

Figure 7(a) presents the development of vertical movement of columns #32 (Y2), #50 (Y3), #67 (Y4), #87 (Y5) and #111 (Y6) with time. The column movement was very similar to wall movement, which undulated during excavation. During the excavation of each layer, the wall moved upward after soil removal due to immediate stress release. Then, the vertical column moved downward continuously. The substantial movement was detected in Stage 7 after the excavation reached the designed depth. This is because removing the soil at the bottom of the pit can result in a sudden decrease in the lateral friction force. Another reason is the discharging of deep artesian water in Stage 7 (Fig. 15), which

results in immediate substantial settlements (Fig. 7(a)). Following the soil removal, column heaves may be expected as well. However, the magnitudes of wall heaves at stages 7 and 8 were relatively small as the bottom of excavation had been reached. The soil remaining at the bottom of foundation pits was mudstone which has a very high elastic modulus. After that, the columns gradually settled when the underground structures were constructed. The column settlement overall was comparably small as the excavation depth almost reached the gravel or mudstone (Fig. 3).

Figure 7(b) shows the relationship between the maximum vertical column movement,  $\delta_{cu}$  and the excavation depth,  $H$ . The maximum vertical column movement,  $\delta_{cu}$  is the maximum vertical displacement of the monitored station. Most of the  $\delta_{cu}$  ranged between the lines of  $\delta_{cu} = -0.05\%H$  and  $\delta_{cu} = -0.06\%H$ . Although the vertical movement of all columns was plotted in the same figure, it can still be observed that the vertical movement increased with the development of excavation. By further analysis of the excavations, it was noticed that at the initial 10 m, the vertical column movement is relatively small, which was because the installation of the anchor cable increased the normal force between columns and soil resulting in an increase of friction. However, when the excavation depth increases, the decrease of the friction due to the removal of the soil cannot be overcome by

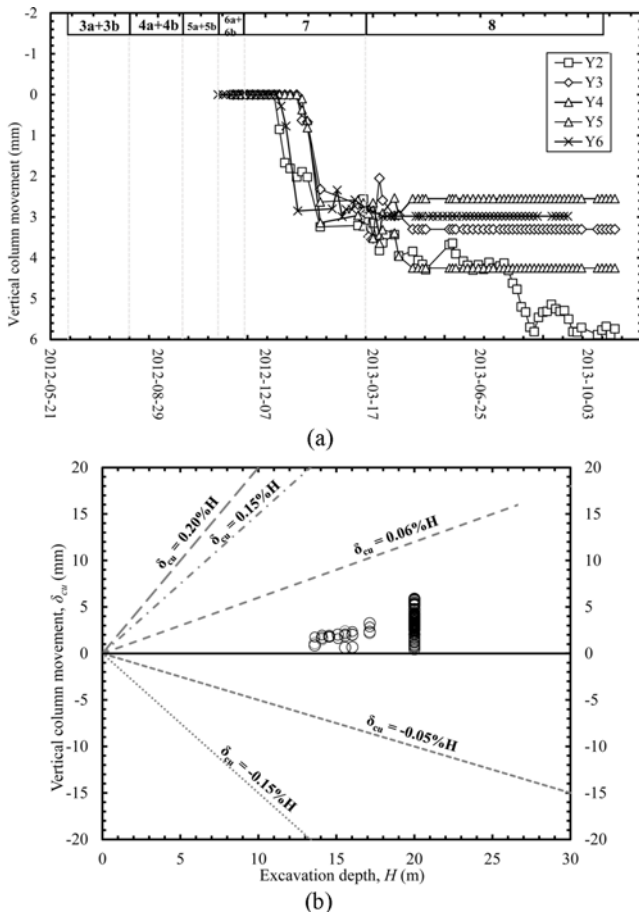


Fig. 7. Typical Development of Column Movement with Time: (a) Vertical Column Movement, (b) Maximum Vertical Column Movement

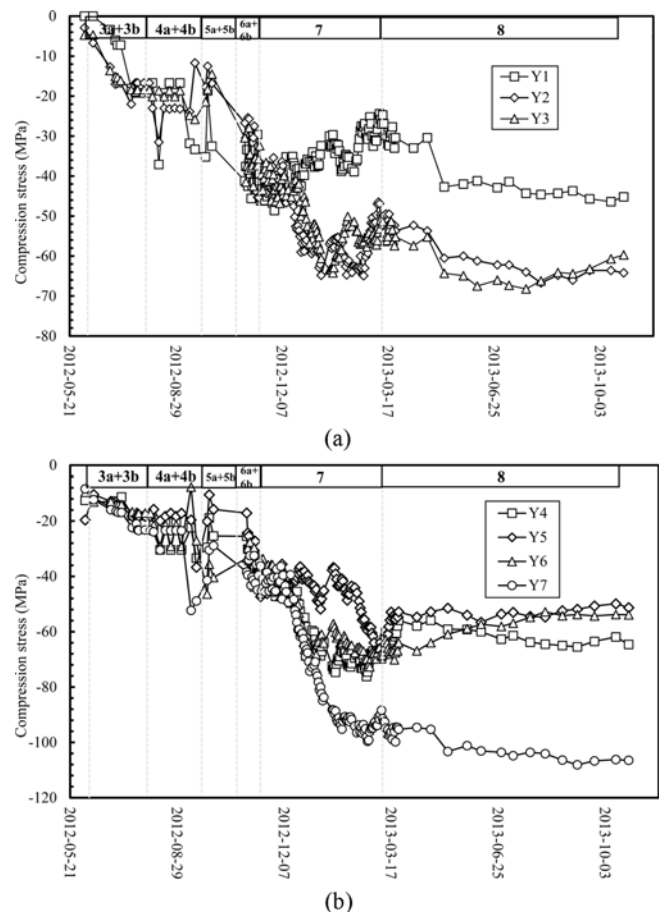


Fig. 8. Typical Development of Column Stress with Time at: (a) East Side of the Pit, (b) North Side of the Pit

the installation of anchor cable resulting in the increase of the column settlement. Another possible reason for the small column movement was due to the stress release of the soil at the basal of the excavation resulting in the rebounding of the soil underneath the column. The lifting up of the column can offset some of the vertical movement of the column. However, the overall settlement was relatively small compared with other soft clay areas (Tan and Wang, 2013b).

Figure 8 presents the development of the stresses during construction in columns located at Y1 – Y7, which were monitored by wire vibrating wire stress meters. Positive values represent tension stress, and negative values represent compression. The instrument was attached to the lower end of the columns. Unlike other excavations, e.g., the cylinder shaft reported by Tan and Wang (2013b), in which the column was in tensile states during most of the excavation time, the columns in this study sustained compression stress. The main reason is that there is no basal heave, and the excavation of soil decreased the surface friction from part of the soil. The self-weight of the column exerted a significant downward load on the interior steel columns, and compression stresses were recorded. The majority of the increase of compression stress was recorded in Stage 7, which corresponded to the period of a rapid drop of artesian water pressure. The drop of water level can cause the dissipation of water in the soils, which means effective stress increases and settlement occurs. Then, a downward force from soil was applied on the columns resulting in the increase of compression stress, as shown in Fig. 8.

The location of the maximum compression stress in the column during excavation is shown in Fig. 9. Although discrepancies existed, the location of the maximum compression stress moved to the bottom of the column. At the very beginning of the excavation, the maximum compression stress was located at the top of the excavation. However, with the development of the excavation, the self-weight of the column cannot be entirely resisted by the skin friction from the surrounding soils. Therefore, bearing force was applied at the end of the columns. Based on force equilibrium, compression stress was observed, and the location of the maximum

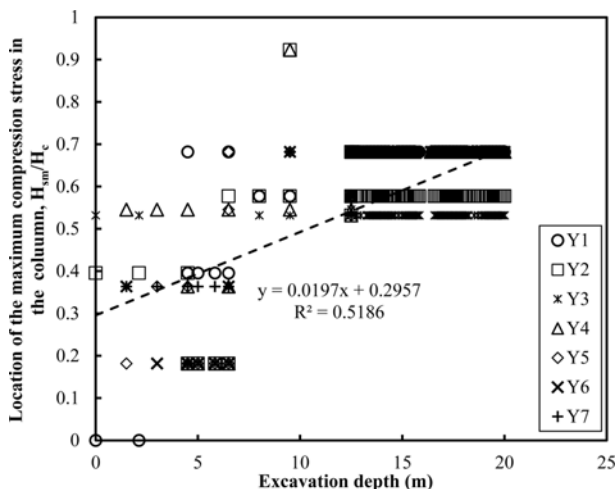


Fig. 9. Variation of the Location of the Recorded Maximum Compression Stress with the Increase of Excavation Depth

stress propagated downward with the proceeding of excavation and pumping. It was also interesting to see that the location of the maximum compression stress was approximately at a depth of excavation, which further verified maximum compression stress resulted from the removal of the soil close to the column in the pit.

### 3.3 Axial Force in the Anchor Cable

Figures 10(a), 10(b) and 10(c) show the typical development of

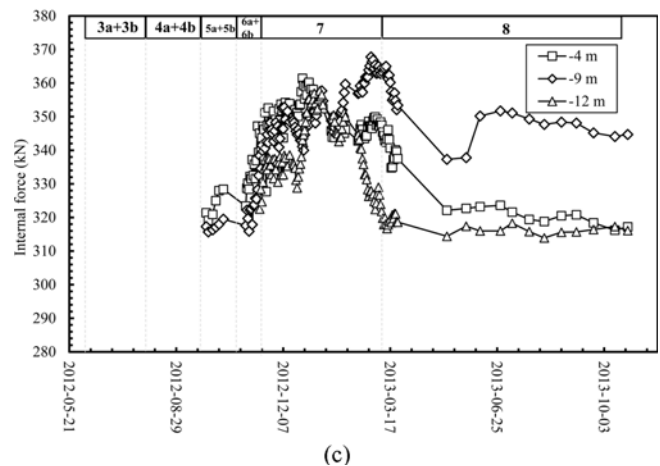
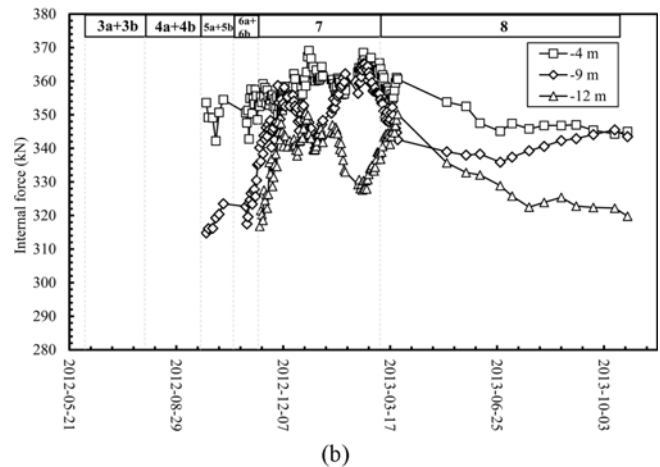
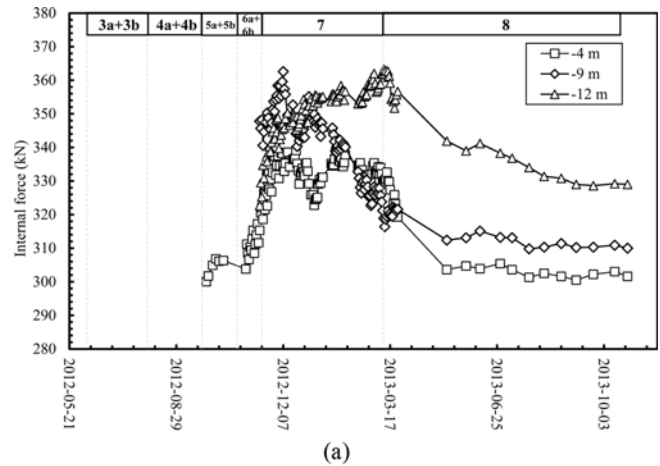


Fig. 10. Development of Internal Force in the Anchor Cables Located at: (a) X2, (b) X5, (c) X7



the measured internal force in the anchor cables at the depths of 4 m, 9 m and 12 m BGS during the excavation. Although the internal force was measured at the north and west of the pit, the overall trend for all three columns was very similar. Based on the available

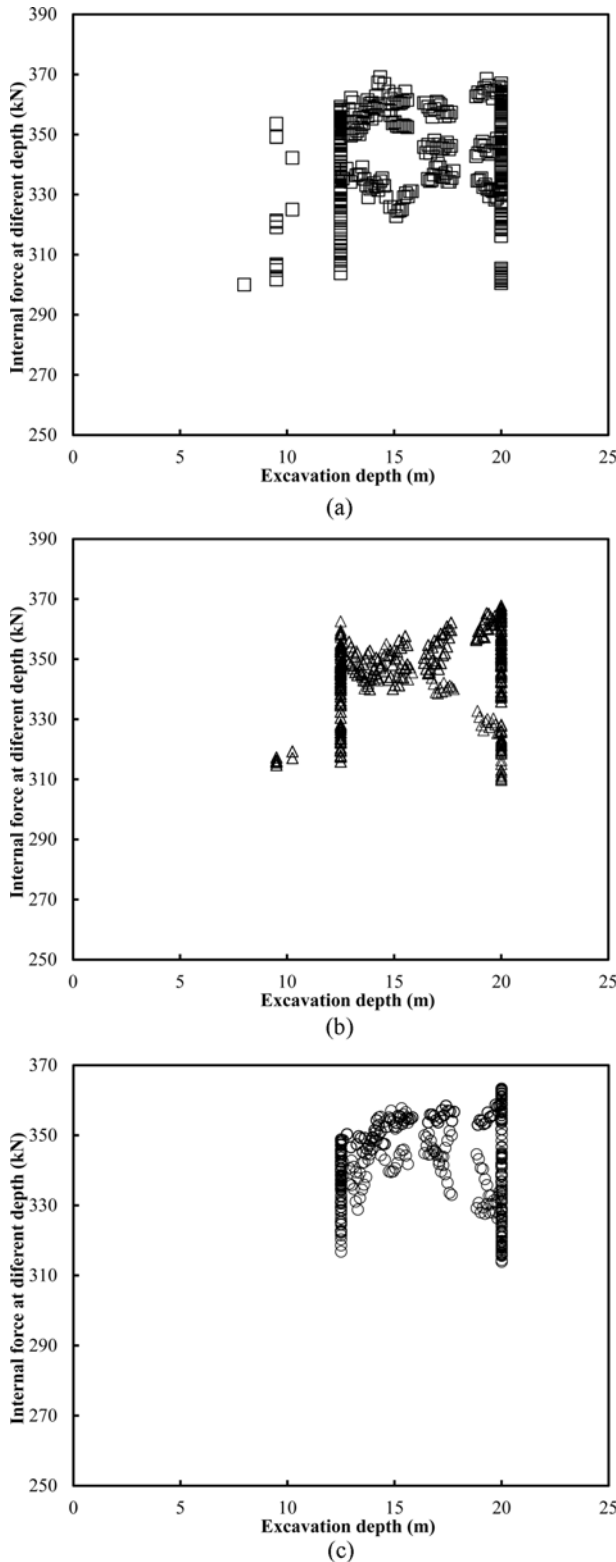


Fig. 11. Excavation Depth, H, vs Internal Force in the Anchor: (a) 4 m BGS, (b) 9 m BGS, (c) 12 m BGS

data, the maximum internal force was observed at Stage 7 when the expected excavation depth was reached, which matched the observed lateral deflection (Fig. 4). It was also interesting to see that the measured maximum internal force for the columns at different locations was very close as excavation depth and soil profile at these locations were very similar.

In Stage 7, the internal force at three different depths was very close to each other, although differences existed, which increased at Stage 8. In addition, the measured maximum internal forces were detected at different depths, 12 m, 4 m and 9 m, for different columns close to X2, X5 and X7, respectively, which indicate potential maximum deflections at the bottom, top and middle of the column. These different behaviours between columns were mainly attributed to the different thickness of soil layers at different cross-sections. The soil layer with high compression strength and Poisson’s ratio can limit the lateral displacement of the soil, which can affect the deflection of the columns. Therefore, the corresponding internal force at the same location for different columns changed. The increase of internal force in Stage 7 was due to the excavation resulting in the displacement of the column moving to the inside of the pit. However, after the stress of soil due to soil excavation was released and consolidation of the soil behind the columns after pumping was completed, the internal force of the column dropped to approximately the same magnitude of the force before soil removal.

Figures 11(a), 11(b) and 11(c) present the relationship between the internal force of anchor cables and excavation depth. During the removal of soil, the internal force measured in the anchor cable changed in a range of 20 – 30 kN. However, when the excavation reached the desired depth, due to the installation of the anchor and stress release of soil, the internal force varied in a range of 30 – 70 kN. The variation of internal force was smaller when the excavation was relatively shallow, e.g., 12.5 m, than that at a deeper depth, e.g., 20 m. However, due to the limited deformation information of the anchor cables in other excavation pits, empirical correlations cannot be concluded for further analysis.

### 3.4 Ground Settlement

Figure 12 shows the typical ground settlement at the different surfaces of the pit. The measured ground settlements increased almost linearly at the south and west side of the pit (Figs. 12(a) and 12(b)). The settlement at the north side of the pit kept at a constant magnitude after the excavation reached the expected depth (Fig. 12(c)). The measured ground settlement on average was 3 – 5 mm, which was mainly attributed to the small column deflections around the monitoring points. Following the pausing of the dewatering pump, an approximate 1 – 2 mm rebound of ground level was detected at Stage 8 at the south and west sides of the pit (Figs. 12(a) and 12(b)). The small ground settlement compared with other large excavation pits may attribute to the prompt installation of the anchor cables (Tan and Wang, 2013a, 2013b).

The relationship between the maximum ground settlement,

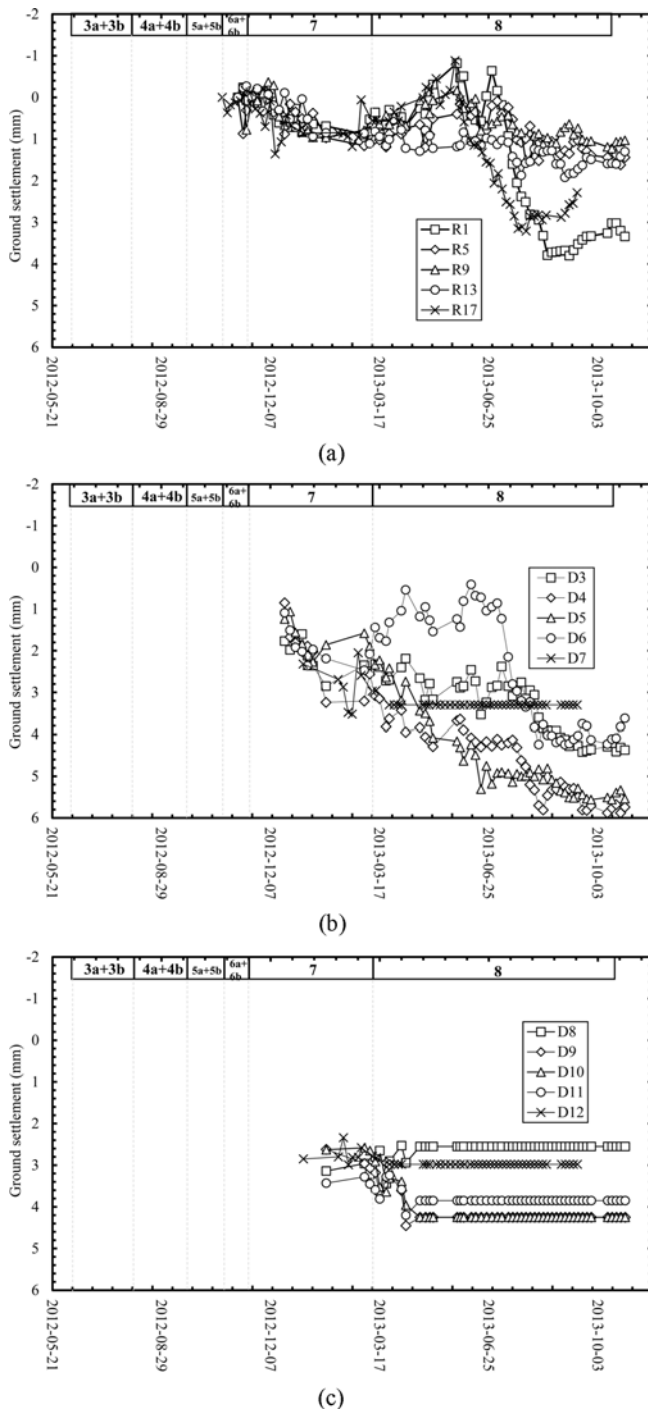


**Fig. 12.** Settlement along the Boundary of the Open Excavation: (a) Along the Railway at the South Side of the Pit, (b) At the West Side of the Pit, (c) At the North Side of the Pit

$\delta_{vm}$ , and the excavation depth,  $H$ , is presented in Fig. 13. The measured  $\delta_{vm}$  was the vertical displacement of the monitored point, which was always the lower boundary proposed by Hashash et al. (2008),  $\delta_{vm} = 0.05\%H$ . Overall, the observed  $\delta_{vm}$  of the excavation studied here was considerably smaller than that proposed by Clough (1990) for excavations in clay (i.e.,  $\delta_{vm} = 0.15\%H$  and  $\delta_{vm} = 0.50\%H$ ). This comparison indicated that

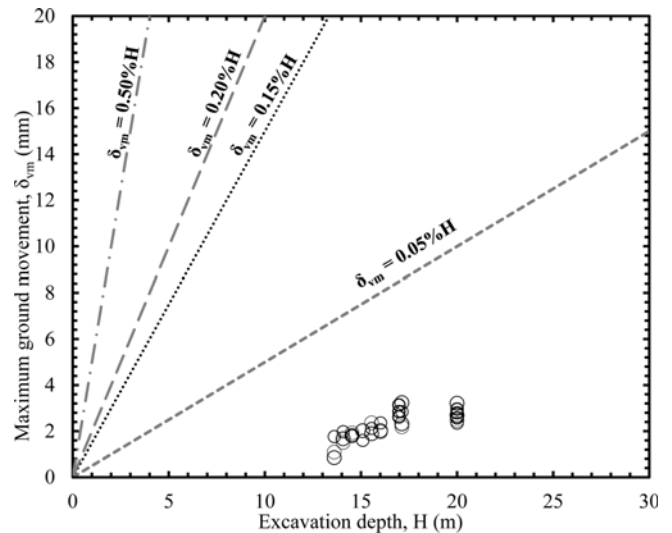


**Fig. 13.** Relationship between Maximum Ground Settlement,  $\delta_{vm}$ , and Excavation Depth,  $H$

the excavation, along with the reasonable reinforced structures, i.e., anchor cables, was capable of limiting the ground settlement than the regular basement pits in terms of the magnitude of settlement. In addition, the small settlement also benefitted from stiff soils, e.g., sand, gravel and sandstone, in the study area, which limited the heaving and settlement of the foundation base.

The ground settlement was measured about 2 m behind the column used to prevent lateral slope failure. When plotting the normalized ground settlement,  $\delta_{vm}/H_c$ , against the normalized distance behind column,  $d/H_c$ , in which  $H_c$  is the final excavation depth, the ground settlement in this study, as expected, was in the stiff clay zone as proposed by Clough (1990), Hashash et al. (2008) and Tan and Wang (2013a). The excavation of CDUTP fell within Zone I in Peck (1969) for the excavation of sand. Different from the observation in Shanghai, China, although the excavation of CDUTP had a very large size, the ground settlement was very small, which resulted from the reinforcement

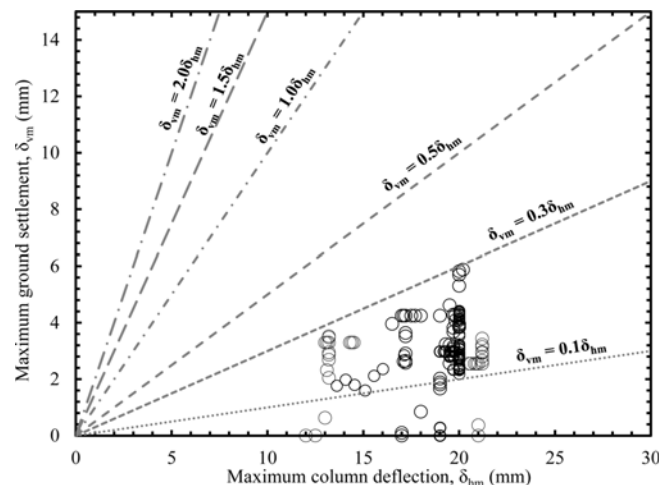


**Fig. 14.** Relationship between Maximum Ground Settlement,  $\delta_{vm}$ , and Maximum Column Deflection,  $\delta_{hm}$

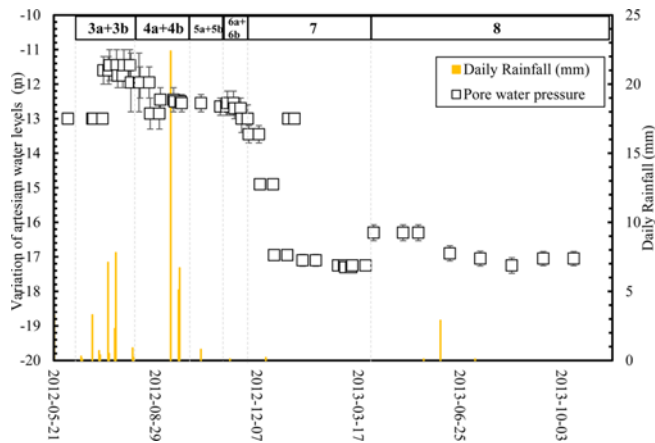


Fig. 15. Variation of the Artesian Water Level during the Construction

during the construction and soil conditions underneath the open pit.

Figure 14 shows the relationship between the maximum wall deflection,  $\delta_{hm}$ , and the corresponding maximum ground settlement,  $\delta_{vm}$ . The observed relationship was between  $\delta_{vm} = 0.1\delta_{hm}$  and  $\delta_{vm} = 0.3\delta_{hm}$ , which were smaller than measured in Shanghai soft clay (Tan and Wang, 2013b). In addition,  $\delta_{vm}/\delta_{hm}$  was also much smaller than that reported by Mana and Clough (1981) and Moormann (2004). Again, the small lateral deflection of the columns limited the ground settlement, which essentially can be attributed to the installation of the anchor cables.

### 3.5 Pore Water Pressure

Since the discharging of artesian water can result in the change of excavation behaviour, the variation of the water level under the ground surface was monitored during the excavation. Fig. 15 indicates the variation of the average artesian water level along with the progress of the excavation, and the error bars show the maximum and minimum water levels around the boundary of the excavation pit during observation. With the development of the excavation, the artesian water level drops accordingly with the help of the pumping. Due to the expected depth was reached in October 2013, the artesian water level dropped suddenly, resulting from the increased pumping rate in a short time. The water level after pumping was kept at a constant level until the end of the excavation. Overall, the artesian water level dropped gently during most of the construction time.

Rainfall can infiltrate into the soil and result in the increase of artesian water level considerably. During the construction stage, the maximum rainfall was 22 mm/day, which happened in stages 4a and 4b. However, the effect of rainfall on the artesian water level was very limited, as shown in Fig. 15. Therefore, the variation of the artesian water level can be attributed to the pumping rate, as stated above.

## 4. Discussion

### 4.1 Empirical Relationships

As the available correlations are mostly developed based on the

shallow excavations, when the correlations developed by Peck (1969), Clough (1990) and Kung et al. (2007) were applied to deep foundations, the correlation does not always match the observed information. By summarizing the deformation characteristics of another seven projects in Chengdu, although discrepancies exist, the relationship between  $\delta_{hm}$  and  $H$  for other cases overall was close to that of CDUTP. When comparing the excavation behaviour of the pits in this study with that in Shanghai (Tan and Wang, 2013b), it was interesting to find that the development of maximum wall deflection with excavation depth in this study (Fig. 5) was very close to the lower boundary proposed by Xu (2007) which was developed based on the excavation of 92 basements in Shanghai. From the comparison of the mechanical properties of soils, it can be concluded that the main reason for the small deflection for CDUTP was due to the high strength of the soil, indicated by the high cohesion of subsurface soil. According to the soil properties reported by Tan and Wang (2013a), the cohesion of subsurface soil was about 20 kPa. However, for subsurface soil in CDUTP, the cohesion was about 40 kPa. Another reason was the installation of the anchor cables, which can effectively limit the movement of the wall.

The maximum column movements observed for CDUTP were less than 5 mm. Compared with the observed column movement for Shanghai World Finance Center (SWFC) (Tan and Wang, 2013a), the observed maximum column movement ranged from 6 mm to 30 mm when an excavation depth of 18 m was reached. There are three reasons that result in the small column movement. The first one is the soil type along the pipe. For the excavation pit reported by Tan and Wang (2013a), the soil along the pile in the vertical direction was clay. However, for CDUTP, the soil along the pile was silt, sand and gravel, which can provide high side friction to the pile. Another reason is the type of column used to limit the soil movement around the excavation pit. For SWFC, H-section steel columns (460 × 460 mm) were used. However, for CDUTP, cylinder concrete pipes with a diameter of 1 m were constructed on-site, which can provide a large side surface. The last reason was mudstone underneath the bottom of the excavation pit, which limited the settlement or bottom heave. Therefore, a small settlement may be expected if the bottom of the excavation is close to bedrock.

A small ground settlement was also measured with a magnitude of 2 mm on average, which was relatively small compared with that reported by Tan and Wang (2013a) for SWFC, 30 – 70 mm. Two main reasons may contribute to the large difference. The first reason was the excavated soil for CDUTP has a higher Young's modulus, 27 – 40 MPa, compared with 10 MPa for SWFC, which can limit the strain under the same normal stress. A portion of the settlement is from the soil underneath the excavation, which is mudstone primarily for CDUTP. Therefore, the settlement for CDUTP is very small. The installation of anchor cable limited the lateral movement of soil as well, which was only 14 – 16 mm. Small lateral movement constrained the soil behind the concrete column, which further limits the settlement of soil in the vertical direction.

## 4.2 Effect of Pit Sizes

Pit size plays a dominant role in the magnitude of wall deflections and ground settlements. The area of the excavation pit of CDUTP is

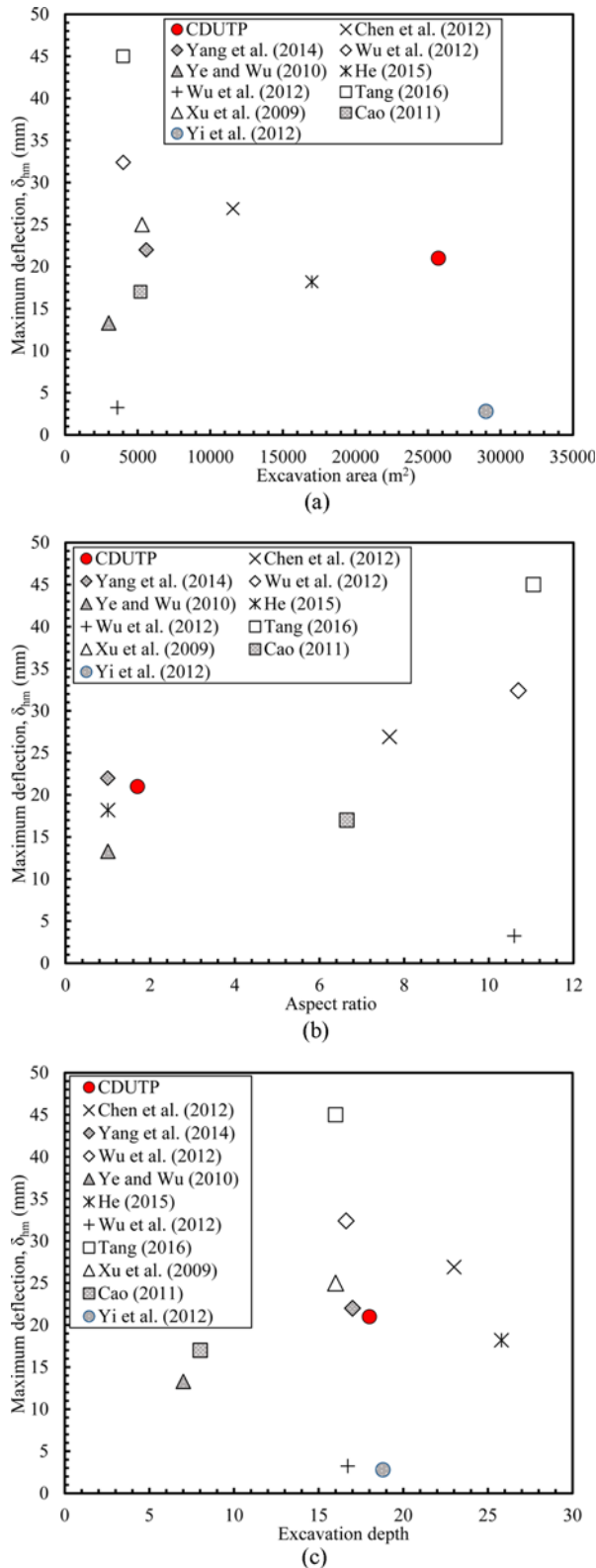


Fig. 16. The Effect of: (a) Pit Size, (b) Aspect Ratio, (c) Excavation Depth on the Maximum Deflection of the Column

25,720  $m^2$  with an aspect ratio of 1.7. It was concluded that larger excavation pits (plane area of 30,000 to 50,000  $m^2$ ) might have three to five times of wall deflections and wall settlements compared with small-scale excavation pits (Tan and Wang, 2013a). As wall settlement is not always reported in the previous publication, maximum deflection on the wall was selected as an index to show the effect of pit size on the foundation excavation. The data from another ten foundation pits in the Chengdu area were also included to study the impact of pit size on excavation behaviour. The excavation area, aspect ratio (length of pit/width of the pit), and excavation depth were investigated.

Figure 16(a) shows that the excavation area of most of the reported foundation pits in the study area were less than 5,000  $m^2$ . For small area excavation, the maximum deflection,  $\delta_{fm}$ , ranged from 3 mm to 45 mm. For the foundation pits with a large area, the maximum deflection was also in this range. It means the maximum deflection is not solely dependent on the excavation area. However, the maximum deflection increased with the aspect ratio (Fig. 16(b)). Although the trend line is with a small value of  $R^2$ , it at least indicates the potential correlation between aspect ratio and maximum deflection. It is also interesting to explore the effect of excavation depth on the maximum deflection. Theoretically, with the increase of excavation depth, the maximum deflection increases as well. The maximum deflection of the reported 11 foundation pits overall follows this trend, although discrepancies exist.

When comparing the wall deflection of the same size excavation pits in other soft clay areas, e.g., Shanghai (Tan and Wang, 2013a), the maximum wall deflection for the same excavation depth is very close. Although different soil properties were reported, the deflection doesn't have a significant difference. However, the ground settlement of CDUTP is smaller than observed in SWFC in Shanghai, which is only 20%–30% of the measured ground settlement. The reason for small ground settlement for CDUTP is attributed to the mechanical properties on soil, which are mostly coarse particles and mudstone at the base of the excavation that can limit the settlement significantly. Therefore, it can be concluded that the pit size can only affect the wall deflection. Ground settlement is still dominated by the soil properties in the excavation pits.

## 4.3 Assessment of Anchor Cables

The lateral deformation of the columns was simulated using Abaqus. Soil properties and thickness in Fig. 3 were used in the simulation. It was shown that the maximum lateral deformation of the columns without installing the anchor cables was approximately close to 65 mm. In comparison, the maximum lateral deflection of the columns stabilized using anchor cables was about 22 mm, 34% of that without anchor cables, which means that the installation of the anchor cables can significantly reduce the lateral deflection.

It was found that a decrease of the prestressing force of 60% can result in a 40% increase of the lateral displacement. And an increase of the prestressing pressure of 60% can cause a decrease

of the lateral displacement by 14%. However, it didn't mean that increasing the prestressing force can continuously reduce lateral displacement, as when the prestress exceeds a threshold value, the lateral displacement will hardly be affected. Therefore, increasing prestressing force of anchor cables to reduce lateral displacement should be chosen with caution. Anchor cables with a prestress of 300 kN were installed during excavation, and the maximum lateral deflection was reduced by 60%. Therefore, it means the design and installation of the anchor cables during this excavation were reasonable.

During this excavation, three to four layers of anchor cables were installed (Table 1). If soil nails along with anchor cables were used during excavation, it was possible to reduce the maximum lateral displacement by 30% to 50% (Chen et al., 2021). It was recommended that decreasing lateral spacing, increasing the number of anchor cables, and the anchor cable's strength can also reduce the lateral displacement by a certain amount (Liu et al., 2021b). In addition, increasing the strength and size of the column was another option to reduce lateral spreading and forces in anchor cables. However, the size and spacing of anchor cables and columns should be optimized based on stability analysis.

## 5. Conclusions

Based on the comprehensive study of the data from the excavation of Chengdu Universal Trade Plaza (CDUTP) foundation pits and comparison of this study to another ten excavations in Chengdu, we can make the following conclusions:

1. Comparing with excavation area, the aspect ratio and excavation depth have a significant effect on the maximum deflection. However, the effect of the excavation area cannot be ignored.
2. The measured wall deflection ranged between  $\delta_{hm} = 0.02\%H$  and  $\delta_{hm} = 0.25\%H$  for this large-scale pit with an area of 25,720 m<sup>2</sup>. The trend line for this case fell between  $\delta_{hm} = 0.1\%H$  and  $\delta_{hm} = 0.15\%H$ . The measured  $\delta_{hm}$  in this study was even smaller than the lower boundaries proposed by Clough (1990) ( $\delta_{hm} = 0.22\%H$ ), and Kung et al. (2007) ( $\delta_{hm} = 0.2\%H$ ).
3. The vertical column movement,  $\delta_{cu}$ , undulated during excavation. After the expected depth was reached, the increase in the vertical column movement was negligible. The vertical column movement ranges between  $\delta_{cu} = 0$  and  $\delta_{cu} = 0.06\%H$ , which is relatively small, resulting from the soil conditions close to the bottom of the excavation, where mudstone was detected.
4. The internal force in the anchor cable varied between 20 – 30 kN during the excavation and between 30 – 70 kN when an expected depth was reached. However, empirical correlations are not available to evaluate the magnitude of the internal force.
5. The measured maximum ground settlement,  $\delta_{vm}$ , was always under the line of  $\delta_{vm} = 0.05\%H$ , which was the lower boundary proposed by Hashash et al. (2008), which was also smaller than the lower boundary proposed by Clough (1990) for excavations in clay. When correlate the maximum wall deflection,  $\delta_{hm}$ , and the corresponding maximum ground settlement,  $\delta_{vm}$ , it was observed that observed relationship between  $\delta_{vm}$  and  $\delta_{hm}$ , was between  $\delta_{vm} = 0.1\delta_{hm}$  and  $\delta_{vm} = 0.3\delta_{hm}$ , which were smaller than measured in Shanghai soft clay (Tan and Wang, 2013a). In addition,  $\delta_{vm}/\delta_{hm}$  was also much smaller than that reported by Mana and Clough (1981) and Moormann (2004).
6. The presented result in this paper indicates that deformation characteristics of the foundation pit, e.g., lateral wall deflection, vertical column movement and ground settlement, are dependent on supporting system, i.e., anchor cables, and soil condition, such as mudstone at the bottom of the excavation for this study, resulting in a relatively small movement for columns and ground surface.

## Acknowledgments

Not Applicable

## ORCID

Chao Kang  <https://orcid.org/0000-0003-1963-257X>

## References

- Cao SW (2011) Study on monitoring technology for joint super large and deep foundation pit of national railway and subway at Chengdu east station and its application. *Building Construction* 33(2):94-97 (in Chinese)
- Chen ZC, Mao JQ, Liu JG (2012) Research on displacement and stress of soldier pile structure in foundation pit of metro station in Chengdu. *Tunnel Construction* 32(3):309-314 (in Chinese)
- Chen A, Wang Q, Chen Z, Chen J, Chen Z, Yang J (2021) Investigating pile anchor support system for deep foundation pit in a congested area of Changchun. *Bulletin of Engineering Geology and the Environment* 80(2):1125-1136, DOI: 10.1007/s10064-020-01985-7
- Clough GW (1990) Construction induced movements of in situ walls. Design and performance of earth retaining structures. ASCE Special Conference, Ithaca, NY, USA, 439-470
- Clough GW, Hansen LA (1981) Clay anisotropy and braced wall behavior. *Journal of the Geotechnical Engineering Division* 107(7): 893-913, DOI: 10.1016/0022-1694(81)90218-3
- Eid HT, Alansari OA, Odeh AM, Nasr MN, Sadek HA (2009) Comparative study on the behavior of square foundations resting on confined sand. *Canadian Geotechnical Journal* 46(4):438-453, DOI: 10.1139/T08-134
- Finno RJ, Atmatzidis DK, Perkins SB (1989) Observed performance of a deep excavation in clay. *Journal of Geotechnical Engineering* 115(8):1045-1064, DOI: 10.1061/(ASCE)0733-9410(1989)115:8(1045)
- Fu GQ, Lu JX, Yang J (2010) The application study of support for Chengdu clay foundation pits. *Acta Geologica Sinica* 30(2):225-228 (in Chinese)
- Gao S (2017) Analysis on deformation behavior of the subway foundation pit in cobble stratum in Chengdu area. MSc Thesis, Southwest Jiaotong University, Chengdu, China (in Chinese)

- Hashash YM, Marulanda C, Ghaboussi J, Jung S (2006) Novel approach to integration of numerical modeling and field observations for deep excavations. *Journal of Geotechnical and Geoenvironmental Engineering* 132(8):1019-1031, DOI: 10.1061/(ASCE)1090-0241(2006)132:8(1019)
- Hashash YM, Whittle AJ (1996) Ground movement prediction for deep excavations in soft clay. *Journal of Geotechnical Engineering* 122(6):474-486, DOI: 10.1061/(ASCE)0733-9410(1996)122:6(474)
- Hashash YM, Osouli A, Marulanda C (2008) Central artery/tunnel project excavation induced ground deformations. *Journal of Geotechnical and Geoenvironmental Engineering* 134(9):1399-1406, DOI: 10.1061/(ASCE)1090-0241(2008)134:9(1399)
- He R (2015) Study on deep excavation technology of the Yin Tai Center. MSc Thesis, Xihua Univeristy, Chengdu, China (in Chinese)
- Hsieh PG, Ou CY (1998) Shape of ground surface settlement profiles caused by excavation. *Canadian Geotechnical Journal* 35(6):1004-1017, DOI: 10.1139/t98-056
- Kung GT, Juang CH, Hsiao EC, Hashash YM (2007) Simplified model for wall deflection and ground-surface settlement caused by braced excavation in clays. *Journal of Geotechnical and Geoenvironmental Engineering* 133(6):731-747, DOI: 10.1061/(ASCE)1090-0241(2007)133:6(731)
- Kung GTC, Ou CY, Juang CH (2009) Modeling small-strain behavior of Taipei clays for finite element analysis of braced excavations. *Computers and Geotechnics* 36(1-2):304-319, DOI: 10.1016/j.compgeo.2008.01.007
- Li Z (2012) Study on deformation behavior and its impact factors of deep foundation pit supported by pile anchorage in construction site of complicated geological conditions. MSc Thesis, Chongqing Univeristy, Chongqing, China (in Chinese)
- Liu J, Luo J, Wu K, Zhou H (2021a) 3D numerical analysis of force and deformation characteristics of double-row round piles with anchor cables based on field monitoring data. 2021 2nd international conference on urban engineering and management science (ICUEMS), January 29-31, Sanya, China, 214-218
- Liu L, Wu R, Congress SSC, Du Q, Cai G, Li Z (2021b) Design optimization of the soil nail wall-retaining pile-anchor cable supporting system in a large-scale deep foundation pit. *Acta Geotechnica* 16:2251-2274, DOI: 10.1007/s11440-021-01154-4
- Mana AI, Clough GW (1981) Prediction of movements for braced cuts in clay. *Journal of the Geotechnical Engineering Division* 107(6):759-777, DOI: 10.1061/AJGEB6.0001150
- Moormann C (2004) Analysis of wall and ground movements due to deep excavations in soft soil based on a new worldwide database. *Soils and Foundations* 44(1):87-98, DOI: 10.3208/sandf.44.87
- Ng CW, Shi J, Hong Y (2013) Three-dimensional centrifuge modelling of basement excavation effects on an existing tunnel in dry sand. *Canadian Geotechnical Journal* 50(8):874-888, DOI: 10.1139/cgj-2012-0423
- Ou CY, Hsieh PG, Chiou DC (1993) Characteristics of ground surface settlement during excavation. *Canadian Geotechnical Journal* 30(5):758-767, DOI: 10.1139/t93-068
- Peck RB (1969) Deep excavation and tunneling in soft ground. State-of-the-art-report. Proceedings of 7th international conference on soil mechanics and foundation engineering, August 25-29, Mexico City, Mexico, 225-290
- Takemura J, Kondoh M, Esaki T, Kouda M, Kusakabe O (1999) Centrifuge model tests on double propped wall excavation in soft clay. *Soils and Foundations* 39(3):75-87, DOI: 10.3208/sandf.39.3\_75
- Tan Y, Wang D (2013a) Characteristics of a large-scale deep foundation pit excavated by the central-island technique in Shanghai soft clay. II: Top-down construction of the peripheral rectangular pit. *Journal of Geotechnical and Geoenvironmental Engineering* 139(11):1894-1910, DOI: 10.1061/(ASCE)GT.1943-5606.0000929
- Tan Y, Wang D (2013b) Characteristics of a large-scale deep foundation pit excavated by the central-island technique in Shanghai soft clay. I: Bottom-up construction of the central cylindrical shaft. *Journal of Geotechnical and Geoenvironmental Engineering* 139(11):1875-1893, DOI: 10.1061/(ASCE)GT.1943-5606.0000928
- Tang YJ (2016) Chengdu metro jinjiang station deformation prediction research. MSc Thesis, Southwest Jiaotong Univeristy, Chengdu, China (in Chinese)
- Wu LB, Tu X, Zhu J, Yuan P (2012) The time-space effect analysis on lateral displacement of a deep-foundation pit in Chengdu. *Construction & Design for Project 2*:101-104 (in Chinese)
- Xu ZH (2007) Deformation behavior of deep excavations supported by permanent structures in Shanghai soft deposit. PhD Thesis, Shanghai Jiao Tong University, Shanghai, China
- Xu XT, Wang JL, Zhao GC (2009) Stability monitoring and analysis of deep foundation pit in excavation. *Sichuan Building Science* (4):124-127 (in Chinese)
- Yang Q, Qian X, Zhu LH, Fan KQ, Chen HX (2014) Numerical simulation and field monitoring of pile anchor supporting structure in deep excavation in Chengdu. *Soil Engineering and Foundation* 28(2):75-79 (in Chinese)
- Ye Q, Wu QL (2010) Monitoring analysis and deformation characteristics of a deep foundation pit. *Chinese Journal of Geotechnical Engineering* 32(S2):541-544 (in Chinese)
- Yi Y, Meles D, Nassiri S, Bayat A (2015) On the compressibility of tire-derived aggregate: Comparison of results from laboratory and field tests. *Canadian Geotechnical Journal* 52(4):442-458, DOI: 10.1139/cgj-2014-0110
- Yi T, Yang W, Bao YW, Liu XH (2012) Research on influence of excavation of foundation pit in capitamalls (Chengdu) Tianfu project on bridge pile foundation. *Subgrade Engineering* 3:84-87 (in Chinese)
- Yu Y (2012) Study of displacement of a typical deep foundation in Chengdu area. *Sichuan Architecture* 32(6):71-73 (in Chinese)
- Zhang S, Pei X, Wang S, Huang R, Zhang X (2020) Centrifuge model testing of loess landslides induced by excavation in northwest China. *International Journal of Geomechanics* 20(4):04020022, DOI: 10.1016/j.enggeo.2019.105170